

## Rates of Oxygen-Isotope Exchange between Sites in the $[\text{H}_x\text{Ta}_6\text{O}_{19}]^{(8-x)-}(\text{aq})$ Lindqvist Ion and Aqueous Solutions: Comparisons to $[\text{H}_x\text{Nb}_6\text{O}_{19}]^{(8-x)-}(\text{aq})$

Edina Balogh,<sup>†‡</sup> Travis M. Anderson,<sup>§</sup> James R. Rustad,<sup>†</sup> May Nyman,<sup>§</sup> and William H. Casey<sup>\*†‡</sup>

Departments of Chemistry and Geology, University of California, Davis, California 95616, and Geochemistry Division, Sandia National Laboratories, Albuquerque, New Mexico 87185

Received May 2, 2007

Rates of steady oxygen-isotope exchange differ in interesting ways for two sets of structural oxygens in the  $[\text{H}_x\text{Ta}_6\text{O}_{19}]^{(8-x)-}(\text{aq})$  Lindqvist ion when compared to published data on the  $[\text{H}_x\text{Nb}_6\text{O}_{19}]^{(8-x)-}(\text{aq})$  version. Because of the lanthanide contraction, the  $[\text{H}_x\text{Ta}_6\text{O}_{19}]^{(8-x)-}(\text{aq})$  and  $[\text{H}_x\text{Nb}_6\text{O}_{19}]^{(8-x)-}(\text{aq})$  ions are virtually isostructural and differ primarily in a full core (Kr vs Xe) and the  $4f^{14}$  electrons in the  $[\text{H}_x\text{Ta}_6\text{O}_{19}]^{(8-x)-}(\text{aq})$  ion. For both molecules, both pH-dependent and -independent pathways are evident in isotopic exchange of the 12  $\mu_2\text{-O}(\text{H})$  and 6  $\eta\text{=O}$  sites. Rate parameters for  $\eta\text{=O}$  exchange at conditions where there is no pH dependence are, for the Ta(V) and Nb(V) versions respectively,  $k_0^{298} = 2.72 \times 10^{-5} \text{ s}^{-1}$  and  $9.7 \times 10^{-6} \text{ s}^{-1}$ ,  $\Delta H^\ddagger = 83.6 \pm 3.2$  and  $89.4 \text{ kJ}\cdot\text{mol}^{-1}$ , and  $\Delta S^\ddagger = -51.0 \pm 10.6$  and  $-42.9 \text{ J}\cdot\text{mol}^{-1}\cdot\text{K}^{-1}$ . For the  $\mu_2\text{-O}$  sites,  $k_0^{298} = 1.23 \times 10^{-6} \text{ s}^{-1}$ ,  $\Delta H^\ddagger = 70.3 \pm 9.7$  and  $88.0 \text{ kJ}\cdot\text{mol}^{-1}$ , and  $\Delta S^\ddagger = -116.1 \pm 32.7$  and  $-29.4 \text{ J}\cdot\text{mol}^{-1}\cdot\text{K}^{-1}$ . Protonation of the 6  $\eta\text{=O}$  sites is energetically unfavored relative to the 12  $\mu_2\text{-O}$  bridges in both molecules, although not equally so. Experimentally, protonation labilizes both the  $\mu_2\text{-O}(\text{H})$  and  $\eta\text{=O}$  sites to isotopic exchange in both molecules. Density-functional electronic-structure calculations indicate that proton affinities of structural oxygens in the two molecules differ with the  $[\text{H}_x\text{Ta}_6\text{O}_{19}]^{(8-x)-}(\text{aq})$  anion having a smaller affinity to protonate than the  $[\text{H}_x\text{Nb}_6\text{O}_{19}]^{(8-x)-}(\text{aq})$  ion. This difference in proton affinities is evident in the solution chemistry as  $\text{p}K_a = 11.5$  for the  $[\text{HTa}_6\text{O}_{19}]^{7-}(\text{aq})$  ion and  $\text{p}K_a = 13.6$  for the  $[\text{HNb}_6\text{O}_{19}]^{7-}(\text{aq})$  ion. Most striking is the observation that  $\eta\text{=O}$  sites isotopically equilibrate faster than the  $\mu_2\text{-O}$  sites for the  $[\text{H}_x\text{Ta}_6\text{O}_{19}]^{(8-x)-}(\text{aq})$  Lindqvist ion but slower for the  $[\text{H}_x\text{Nb}_6\text{O}_{19}]^{(8-x)-}(\text{aq})$  ion, indicating that predictions about site reactivities in complicated structures, such as the interface of aqueous solutions and oxide solids, should be approached with great caution.

### Introduction

The early transition metals in their high oxidation states form multimetric metal oxide clusters, called polyoxometalates, in aqueous solutions. These structures are enormously useful for a myriad of processes in inorganic chemistry, material science, medicine, and environmental chemistry.<sup>5–9</sup> Although there is much research on these polyoxometalates,

relatively little is known about the pathways by which they react and transform in an aqueous solution,<sup>10</sup> yet this information not only would be useful to polyoxometalate researchers but also would be extraordinarily helpful to scientists trying to understand how larger extended oxide materials such as catalyst supports and clays react in water.

\* To whom correspondence should be addressed. E-mail: whcasey@ucdavis.edu. Phone: 530-752-3211.

<sup>†</sup> Department of Chemistry, University of California.

<sup>‡</sup> Department of Geology, University of California.

<sup>§</sup> Sandia National Laboratories.

- (1) Nyman, M.; Alam, T. M.; Bonhomme, F.; Rodriguez, M. A.; Frazer, C. S.; Welk, M. E. *J. Cluster Sci.* **2006**, *17* (2), 197–204.
- (2) Etxebarria, N.; Fernandez, L. A.; Madariaga, J. M. *J. Chem. Soc., Dalton Trans.* **1994**, *20*, 3055–3059.
- (3) Anderson, T. M.; Alam, T. M.; Bonhomme, F.; Rodriguez, M. A.; Nyman, M. *Dalton Trans.* **2007**, in press.

(4) Black, J. R.; Nyman, M.; Casey, W. H. *J. Am. Chem. Soc.* **2006**, *128* (45), 14712–14720.

(5) Hill, C. L. *J. Mol. Catal. A: Chem.* **2007**, *262* (1–2), 2–6.

(6) Long, D.-L.; Burkholder, E.; Cronin, L. *Chem. Soc. Rev.* **2007**, *36* (1), 105–121.

(7) Katsoulis, D. E. *Chem. Rev. (Washington, DC, U.S.)* **1998**, *98* (1), 359–387.

(8) Rhule, J. T.; Hill, C. L.; Judd, D. A.; Schinazi, R. F. *Chem. Rev. (Washington, DC, U.S.)* **1998**, *98* (1), 327–357.

(9) Müller, A.; Peters, F.; Pope, M. T. *Chem. Rev. (Washington, DC, U.S.)* **1998**, *98* (1), 239–271.

(10) Hill, C. L. *Compr. Coord. Chem. II* **2004**, *4*, 679–759.

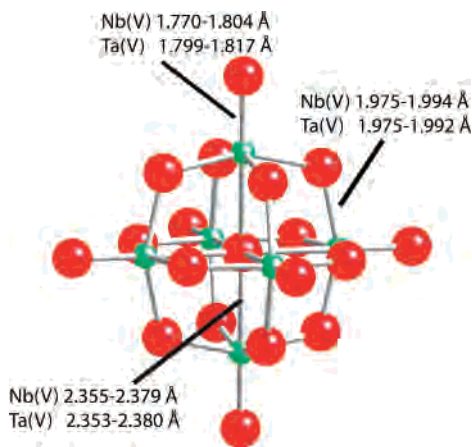


**Figure 1.** Lindqvist ions having a central  $\mu_6$ -O site that is inert to exchange, 12  $\mu_2$ -O bridges, and 6 terminal  $\eta$ =O sites. In the ball-and-stick representation, the oxygens are red and the metals [either Ta(V) or Nb(V)] are green. The bond lengths were determined from X-ray structures of the alkali-metal salts of the Nb(V) and Ta(V) Lindqvist ions in various stoichiometries<sup>1,3</sup> (Table S-4 in the Supporting Information).

Because the polyoxometalate molecules are nanometer in scale and absolutely discrete in size and geometry, experimental data on steady oxygen-isotope-exchange reactions could be easily complemented with density functional theory (DFT) or molecular dynamics simulations to provide real insight into elementary, or near-elementary, reaction pathways<sup>11</sup> and recently for the Nb(V) Lindqvist ion.<sup>4</sup>

The Lindqvist ions comprise one of the simplest classes of polyoxometalates (Figure 1) because they consist of a superoctahedron of 6  $M(O)_6$  octahedra that are linked by 12  $\mu_2$ -O(H) bridges at a  $\mu_6$ -O; each of the six metals is terminated by a  $\eta$ =O. The Lindqvist ion has an internal structural oxygen ( $\mu_6$ -O) that is inert to exchange,<sup>1,4,12–17</sup> and the constant  $^{17}\text{O}$  NMR signal from this  $\mu_6$ -O indicates that the ion remains intact in solution as the other structural oxygens isotopically equilibrate with bulk water. Using this method, in earlier work we studied isotope exchange in the  $[\text{HNb}_6\text{O}_{19}]^{7-}$  Lindqvist ion<sup>4</sup> and found that, at pH  $\sim$  11.5–14, the 12  $\mu_2$ -O(H) bridges exchange about  $\sim$ 10 times faster than the  $\eta$ =O sites but, at lower or higher pH values, these two oxygen sites can react at identical rates.<sup>1,12–17</sup>

In this paper, we expand this work and report the rates of isotopic equilibration of the Ta(V) version of this Lindqvist ion. Because of the lanthanide contraction, the Ta(V) and Nb(V) versions of the Lindqvist ions are nearly isostructural. Metals in the two structures have a closed-shell electronic configuration (Xe and Kr, respectively) and primarily differ by the full shell of  $4f^{14}$  electrons in the Ta(V) version of the

Lindqvist ion. Nevertheless, we show that these molecules react profoundly differently with an aqueous solution in ways that challenge and enrich our understanding of the reaction pathways in aqueous solutions.

## Methods

### Synthesis of the $^{17}\text{O}$ -Enriched $[\text{Ta}_6\text{O}_{19}]^{8-}$ Starting Material.

Details of the synthesis will be presented in another work and will not be reviewed extensively here. Briefly, a  $\text{NaK}_7[\text{Ta}_6\text{O}_{19}] \cdot 14\text{H}_2\text{O}$  salt was made by catalyzed decomposition of  $\text{K}_3\text{Ta}(\text{O}_2)_4$  in a basic solution that also contains  $^{17}\text{O}$ -enriched water. The resulting solution was slowly evaporated in the presence of KOH to yield crystals of  $^{17}\text{O}$ -enriched salts. Most experiments were conducted from a single 2.76 g batch of  $\text{NaK}_7[\text{Ta}_6^{17}\text{O}_{19}] \cdot 14\text{H}_2\text{O}$  salt. For this particular synthesis, a 4.00 g (9.4 mmol) sample of  $\text{K}_3\text{TaO}_8$ , 3.83 g (68 mmol) of KOH, and 0.137 g (0.6 mmol) of  $\text{K}_3\text{VO}_4$  were added to 10 mL of water (20%  $^{17}\text{O}$ ), and the mixture was refluxed and stirred until a clear solution was obtained ( $\sim$ 30–45 min). The warm solution was filtered with a 0.45  $\mu\text{m}$  syringe, and 2.76 g of crystalline material was obtained by slow evaporation of the solution at room temperature over 2 days (91% yield). The  $^{17}\text{O}$  NMR spectrum of the sample indicates a ratio of peak intensities for the  $\mu_6$ -O,  $\eta$ =O, and  $\mu_2$ -O sites of 1:6:12, as is expected from the molecule's stoichiometry.

**Rate Measurements.** An experiment was typically begun by dissolving a few tens of milligrams of the  $\text{NaK}_7[\text{Ta}_6^{17}\text{O}_{19}] \cdot 14\text{H}_2\text{O}$  salt into 1 aliquot of an isotopically normal background electrolyte solution. At 25  $^\circ\text{C}$ , the pH of the resulting self-buffered solution was about 11.5, which is significantly lower than the pH of a corresponding solution made from the  $[\text{Nb}_6\text{O}_{19}]^{8-}$  anion, which was typically at pH  $\sim$  12.4.<sup>4</sup> Other pH conditions were reached by adding either a small amount of 3 M KOH to raise the pH or small amounts of  $\text{K}_2\text{CO}_3$  or  $\text{KHCO}_3$  to lower the pH. These buffers were found previously to have no or little interaction with the Nb(V) Lindqvist ion, which, of course, is anionic.<sup>4</sup> The ionic strength was maintained nearly constant at 3 M with KCl. The pH-adjusted solutions were typically prepared ahead of time, and the salt was dissolved into them at temperature.

The pH of each sample was measured on a concentration scale using a glass combination electrode. The electrode was calibrated by Gran titration using a 3 M KCl solution and a 0.1 M standardized acid at the corresponding temperature. The measured values agree well with those calculated using the concentration of the excess hydroxide ion.

**NMR Spectroscopy.** Variable-temperature  $^{17}\text{O}$  NMR measurements were carried out using a 10-mm broad-band probe on an 11.7 T magnet ( $\nu_0 = 67.8$  MHz for  $^{17}\text{O}$ ) Bruker Avance spectrometer located at the UCD NMR facility. The spectra were taken with single-pulse excitation using 20  $\mu\text{s}$  pulses ( $\pi/2 \approx 40$   $\mu\text{s}$ ) and recycle delays of 6 ms. The number of acquisitions typically varied between 1000 and 10 000 with the sample concentration to obtain an adequate signal-to-noise ratio. The time-domain data were digitized at 100 kHz. In order to prevent corrosion of the glass, we used a Teflon insert fitted into the 10 mm NMR tubes. Although this insert prevented corrosion of the glass, it did allow  $\text{CO}_2$  to enter the solutions, which was detectable as a slow pH drift in the long-term experiments. The temperature was measured by replacing the sample with a solution of background electrolyte containing a copper–constantan thermocouple fitted into the NMR tube. The accuracy of the measured temperature was about  $\pm 0.1$  K.

- (11) Casey, W. H. *Chem. Rev. (Washington, DC, U.S.)* **2006**, *106* (1), 1–16.
- (12) Alam, T. M.; Nyman, M.; Cherry, B. R.; Segall, J. M.; Lybarger, L. E. *J. Am. Chem. Soc.* **2004**, *126* (17), 5610–5620.
- (13) Day, V. W.; Klemperer, W. G. *Science (Washington, DC, U.S.)* **1985**, *228* (4699), 533–541.
- (14) English, A. D.; Jesson, J. P.; Klemperer, W. G.; Mamouneas, T.; Messerle, L.; Shum, W.; Tramontano, A. *J. Am. Chem. Soc.* **1975**, *97* (16), 4785–4786.
- (15) Filowitz, M.; Ho, R. K. C.; Klemperer, W. G.; Shum, W. *Inorg. Chem.* **1979**, *18* (1), 93–103.
- (16) Klemperer, W. G. *Inorg. Synth.* **1990**, *27*, 71–74.
- (17) Klemperer, W. G. *NATO ASI Ser., Ser. C* **1983**, *103* (Multinuclear Approach to NMR Spectroscopy), 245–260.

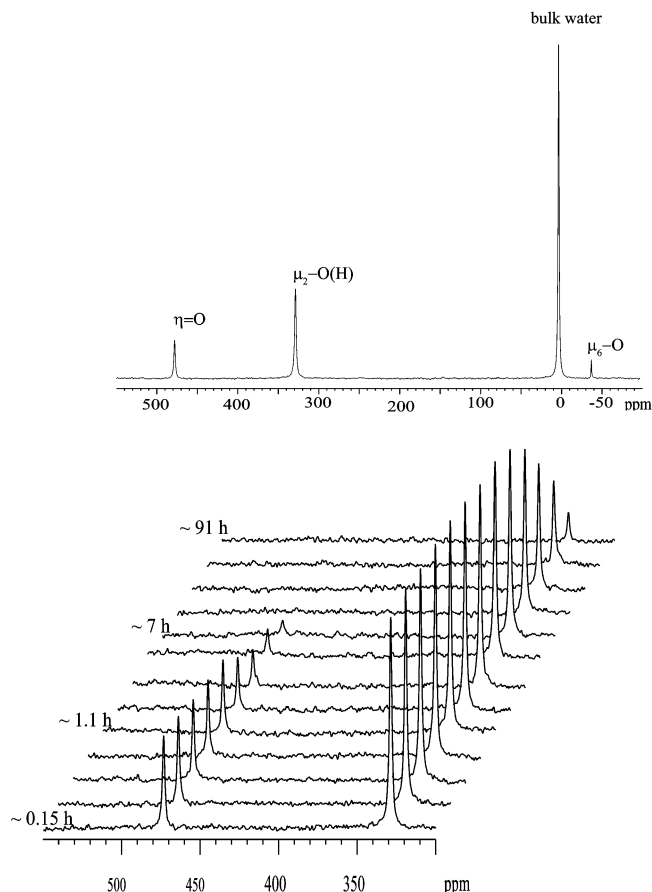


**Figure 2.** (top)  $^{17}\text{O}$  NMR peaks assigned to  $\mu_2\text{-O(H)}$  (top,  $\sim 320$  ppm) and  $\eta=\text{O}$  ( $\sim 470$  ppm), bulk water (0 ppm), and  $\mu_6\text{-O}$  ( $\sim -40$  ppm). The intensity ratios  $\mu_2\text{-O(H)}/\eta=\text{O}/\mu_6\text{-O}$  vary 12:6:1, approximately. (bottom) Successive spectra showing the time variation in the peaks assigned to  $\mu_2\text{-O(H)}$  and  $\eta=\text{O}$  at pH  $\sim 12.8$ .

**DFT Calculations.** The calculations were conducted either by using the conductor-like screening model (COSMO<sup>18</sup>) or by terminating the structures with potassium in order to reduce the anionic charge and maintain the electronic stability.<sup>19</sup> All calculations were conducted using the PQS code from Parallel Quantum Solutions, Inc. (<http://www.pqs-chem.com>). The B3LYP exchange-correlation functional was used, as implemented in the PQS code. The LANL2DZ basis set was chosen for the Nb(V) and Ta(V) metals. This basis set employs an effective core potential that partially takes into account relativistic effects. The basis set 6-31G\* was chosen for the oxygens, potassiums, and hydrogens.

## Results

The  $^{17}\text{O}$  NMR spectrum of the hexatantalate solution contains four conspicuous peaks that are assignable to the  $\eta=\text{O}$  (470–490 ppm),  $\mu_2\text{-O(H)}$  (320–330 ppm), and  $\mu_6\text{-O}$  (near  $-40$  ppm), and the bulk water peak at 0 ppm (Figure 2, top). At the earliest spectrum ( $t_0$  is typically 4–7 min after dissolution of the salt), the integrated areas of the peaks have nearly the ratio of 6:12:1, corresponding to the 6 equivalent  $\eta=\text{O}$  sites, the 12  $\mu_2\text{-O(H)}$  sites, and the single  $\mu_6\text{-O}$  site.

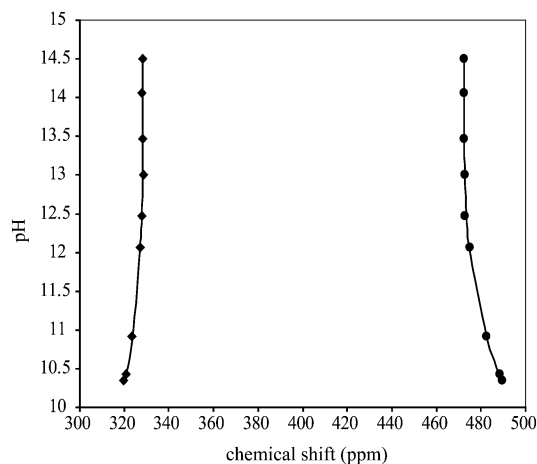


**Figure 3.**  $^{17}\text{O}$  NMR peak positions of  $\eta=\text{O}$  (470–490 ppm) and  $\mu_2\text{-O(H)}$  (320–330 ppm) varying with the pH at constant temperature. Lines are fits of eq 2 to the data, yielding  $\text{p}K_{\text{a}1} = 9.3$  and  $\text{p}K_{\text{a}2} = 11.5$  for the  $[\text{H}_x\text{Ta}_6\text{O}_{19}]^{(8-x)-}$  ion.

These peak assignments agree with those of the previous  $^{17}\text{O}$  NMR spectra of the Ta(V) Lindqvist ions.<sup>14,20</sup>

The  $^{17}\text{O}$  NMR peak positions vary with the pH but not with the temperature in the range we investigated (5.2–48.8 °C), suggesting that protonation equilibrium affects the peak positions. This variation with the pH is important because the acid–base equilibrium constants for the  $[\text{H}_x\text{Ta}_6\text{O}_{19}]^{(8-x)-}$  ion are poorly known, as are the protonation equilibrium constants for Lindqvist ions in general. Because the molecules are so basic, the protonation constants cannot be reliably determined by pH potentiometric titration. The cluster dissociates below pH = 10 and forms a precipitate that limits the pH range that can be investigated. The absorbance of the  $[\text{H}_x\text{Ta}_6\text{O}_{19}]^{(8-x)-}$  ion overlaps with the absorbance of the background electrolyte so that UV–vis spectrophotometry is equivocal.

However, the protonation of different oxygen sites on the  $[\text{H}_x\text{Ta}_6\text{O}_{19}]^{(8-x)-}$  ion apparently leads to a deshielding of peaks (Figure 3) that can allow us to estimate conditional protonation constants. The peak positions,  $\delta_{\text{obs}}$ , can be expressed as

$$\delta_{i,\text{obs}} = \sum_{n=1}^N \delta_{i,\text{H}_n\text{L}} f_{\text{H}_n\text{L}} \quad (1)$$

where  $\delta$  is the intrinsic chemical shift of the  $i$  nucleus of the  $\text{H}_n\text{L}$  species (ppm) and  $f_{\text{H}_n\text{L}}$  is the fractional population of each species. For this calculation, the bulk water peak was set at  $\delta = 0$ . The protonation constants,  $K_{\text{a}}$ , are then related to the  $f_{\text{H}_n\text{L}}$  by

$$K_{\text{a}} = \frac{f_{\text{H}_n\text{L}}}{f_{\text{H}_{n-1}\text{L}}[\text{H}^+]} \quad (2)$$

and optimized via a nonlinear least-squares fitting algorithm to yield  $\text{p}K_{\text{a}1} = 9.3$  and  $\text{p}K_{\text{a}2} = 11.5$  as the most likely values. The pH range investigated was too small to reliably assign

(18) Klamt, A.; Jonas, V.; Buerger, T.; Lohrenz, J. C. W. *J. Phys. Chem. A* **1998**, *102* (26), 5074–5085.

(19) Lopez, X.; Fernandez, J. A.; Romo, S.; Paul, J. F.; Kazansky, L.; Poblet, J. M. *J. Comput. Chem.* **2004**, *25* (12), 1542–1549.

(20) Besecker, C. J.; Klemperer, W. G.; Maltbie, D. J.; Wright, D. A. *Inorg. Chem.* **1985**, *24* (7), 1027–1032.



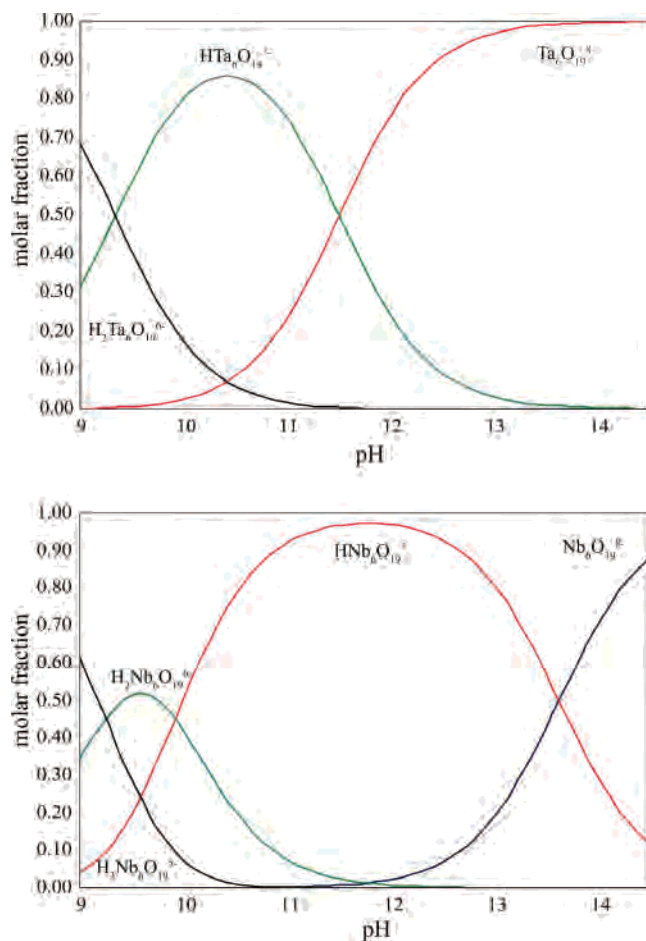


**Figure 4.** Speciation diagram showing the various forms of the  $[\text{H}_x\text{Ta}_6\text{O}_{19}]^{(8-x)-}$  ion ( $x = 0-2$ ) (top) and the  $[\text{H}_x\text{Nb}_6\text{O}_{19}]^{(8-x)-}$  ion ( $x = 0-3$ ) (bottom) in an aqueous solution as a function of the pH at  $I = 3.0 \text{ M}$ . The values of  $\text{p}K_a$  are determined by a least-squares fit to  $^{17}\text{O}$  NMR data (Figure 3). The plot for  $[\text{H}_x\text{Nb}_6\text{O}_{19}]^{(8-x)-}$  employed data from previous work.<sup>2</sup>

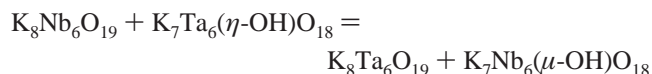
uncertainties to these  $\text{p}K_a$  values, but they allow us to make reasonable estimates of the fraction of various protonated forms of the  $[\text{H}_x\text{Ta}_6\text{O}_{19}]^{(8-x)-}$  ion as a function of the pH (Figure 4). The  $\text{p}K_a$  values for the  $[\text{H}_x\text{Ta}_6\text{O}_{19}]^{(8-x)-}$  ion are somewhat lower than those reported for the  $[\text{H}_x\text{Nb}_6\text{O}_{19}]^{(8-x)-}$  ion ( $\text{p}K_{a1} = 9.35$ ,  $\text{p}K_{a2} = 9.92$ , and  $\text{p}K_{a3} = 13.63$ ).<sup>2,21</sup>

**Calculated Proton Affinities of the Ta(V) and Nb(V) Lindqvist Ions.** As discussed above, the two molecules differ subtly in their solution chemistry as the  $[\text{Ta}_6\text{O}_{19}]^{8-}$  Lindqvist ion is somewhat less basic than the corresponding  $[\text{Nb}_6\text{O}_{19}]^{8-}$  cluster. This difference in acid–base chemistry is manifested in the estimated  $\text{p}K_a$  values as well as in the results of the DFT calculations (see Table S-1 in the Supporting Information).

The DFT calculations indicate clear differences between the two molecules that are consistent with the experiment. It has been shown that electronic energies of isostructural molecules calculated at 0 K are a good indicator of solution  $\text{p}K_a$ .<sup>22,23</sup> The bridging oxo sites have a higher affinity for

protons relative to the terminal  $\text{Nb}(\eta=\text{O})$  and  $\text{Ta}(\eta=\text{O})$  sites, as is common for polyoxometalates where terminal oxygens have higher bond orders than bridging oxygens. Thus, the experimental structures of Ozeki et al.<sup>24</sup> and Nyman et al.<sup>1</sup> show that the protons bond to the bridging oxygens in the niobate cluster. In the solid state, the  $[\text{HTa}_6\text{O}_{19}]^{7-}$  anion has never been crystallized, which is consistent with our observation that the Nb(V) ion is more basic than the Ta(V) Lindqvist ion. All solid-state structures of  $[\text{Ta}_6\text{O}_{19}]$  salts are of the nonprotonated form.<sup>3,25–27</sup>

Almost independent of the position of protonation, a given oxygen in the Nb(V) Lindqvist ion has a consistently higher affinity for protons than that in the corresponding Ta(V) structure. For example, the energies for proton transfer from a bridging oxygen  $[\text{Nb}_6\text{O}_{19}]^{8-} + [\text{Ta}_6(\mu_2\text{-OH})\text{O}_{18}]^{7-} = [\text{Ta}_6\text{O}_{19}]^{8-} + [\text{Nb}_6(\mu_2\text{-OH})\text{O}_{18}]^{7-}$  and  $\text{K}_8\text{Nb}_6\text{O}_{19} + \text{K}_7\text{Ta}_6(\mu_2\text{-OH})\text{O}_{18} = \text{K}_8\text{Ta}_6\text{O}_{19} + \text{K}_7\text{Nb}_6(\mu_2\text{-OH})\text{O}_{18}$  are  $-34$  and  $-23 \text{ kJ}\cdot\text{mol}^{-1}$ , respectively, consistent with bridging oxygens on the Nb(V) Lindqvist ion having a higher proton affinity than those of the corresponding Ta(V) ion. Similar results are achieved regardless of the initial protonation states of the Nb(V) and Ta(V) structures and whether a potassium-terminated cluster or the COSMO solvent model is employed to achieve electronic stability. The one exception is proton transfer between the two  $\eta=\text{O}$  sites:



which has a negligible energy difference.

Because the Nb(V) and Ta(V) molecules have equal preference for a proton at a  $\eta=\text{O}$  site, differences among  $\mu_2\text{-O}$  account for the overall differences in proton affinities between the two molecules. Thus, the energies for reactions  $[\text{Nb}_6(\eta_2\text{-OH})\text{O}_{18}]^{7-} = [\text{Nb}_6(\mu_2\text{-OH})\text{O}_{18}]^{7-}$  and  $[\text{Ta}_6(\eta_2\text{-OH})\text{O}_{18}]^{7-} = [\text{Ta}_6(\mu_2\text{-OH})\text{O}_{18}]^{7-}$  are  $-60$  and  $-45 \text{ kJ}\cdot\text{mol}^{-1}$ , respectively. Corresponding energies for the potassium-terminated structures in the gas phase,  $[\text{K}_7\text{Nb}_6(\eta_2\text{-OH})\text{O}_{18}] = [\text{K}_7\text{Nb}_6(\mu_2\text{-OH})\text{O}_{18}]$  and  $[\text{K}_7\text{Ta}_6(\eta_2\text{-OH})\text{O}_{18}] = [\text{K}_7\text{Ta}_6(\mu_2\text{-OH})\text{O}_{18}]$ , are  $-37$  and  $-15 \text{ kJ}\cdot\text{mol}^{-1}$ . In other words, the energy to move a proton from a bridge to a terminal oxo is always unfavorable but is considerably less unfavorable for the tantalate than for the niobate. Protons lifetimes are undoubtedly less than, or equal to,  $10^{-3} \text{ s}$  on these molecules,<sup>28</sup> which means that the proton will visit all oxygens during the time scale of oxygen-isotope exchange in either molecule, although not to equal extents. As we discuss below, an important experimental observation is that protonation by 2–3 protons apparently labilizes both  $\eta=\text{O}$  and  $\mu_2\text{-O}(\text{H})$  in the clusters, which is surprising.

(21) Rozantsev, G. M.; Dotsenko, O. I.; Taradina, G. V. *Russ. J. Coord. Chem. (Transl. Koord. Khim.)* **2000**, *26* (4), 247–253.

(22) Rustad, J. R.; Dixon, D. A.; Kubicki, J. D.; Felmy, A. R. *J. Phys. Chem. A* **2000**, *104* (17), 4051–4057.

(23) Rustad, J. R.; Dixon, D. A.; Rosso, K. M.; Felmy, A. R. *J. Am. Chem. Soc.* **1999**, *121* (13), 3234–3235.

(24) Ozeki, T.; Yamase, T.; Naruke, H.; Sasaki, Y. *Bull. Chem. Soc. Jpn.* **1994**, *67* (12), 3249–3253.

(25) Hartl, H.; Pickhard, F.; Emmerling, F.; Roehr, C. Z. *Anorg. Allg. Chem.* **2001**, *627* (12), 2630–2638.

(26) Lindqvist, I.; Aronsson, B. *Ark. Kemi* **1953**, *6* (7), 49–52.

(27) Pickhard, F.; Hartl, H. Z. *Anorg. Allg. Chem.* **1997**, *623* (8), 1311–1316.

(28) Houston, J. R.; Phillips, B. L.; Casey, W. H. *Geochim. Cosmochim. Acta* **2006**, *70* (7), 1636–1643.

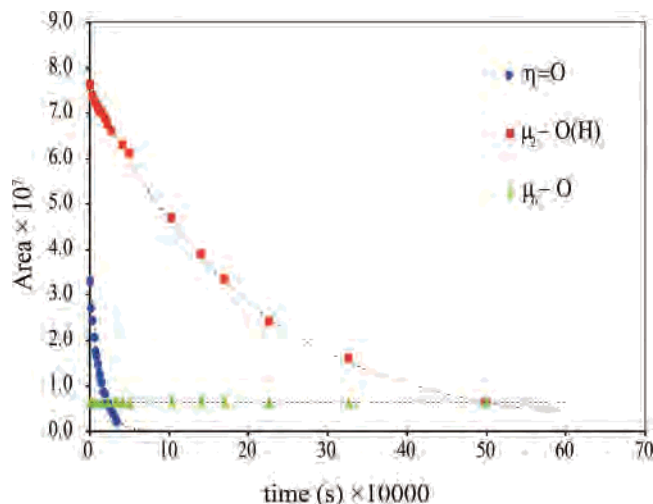


**Figure 5.** Intensity of the  $^{17}\text{O}$  NMR signal in a given peak decreasing exponentially with time. Here the intensities of the  $\eta=\text{O}$  and  $\mu_2\text{-O}$  peaks decrease exponentially, while the signal for the central  $\mu_6\text{-O}$  site is constant, indicating that the molecule remains intact during the reaction. The rate coefficients,  $k_{\text{obs}}$ , and characteristic time,  $\tau = 1/k_{\text{obs}}$ , are determined by a fit of eq 3 to the data. The enriched compound was dissolved in 2 mL of 3 M KOH.

**Oxygen-Isotope-Exchange Rates.** The rates of oxygen-isotope exchange between bulk water and the isotopically enriched  $[\text{H}_x\text{Ta}_6\text{O}_{19}]^{(8-x)-}$  ion were estimated from diminution of the  $^{17}\text{O}$  NMR signal from the  $\eta=\text{O}$  and  $\mu_2\text{-O(H)}$  sites as a function of time. During these experiments, the peaks corresponding to the  $\mu_6\text{-O}$  sites exhibited no appreciable change in intensity, indicating that the molecule remains intact as the isotope-exchange reactions proceed at the other sites (Figures 2 and 5). A typical exponential decay of the peak intensity as a function of time is shown in Figure 5, along with a fit to the data. The pseudo-first-order rate constants ( $k_{\text{obs}}$ ) were calculated by fitting the intensity data to

$$I_t = (I_0 - I_e) \exp(-k_{\text{obs}}t) + I_e \quad (3)$$

where  $I$ ,  $I_0$ , and  $I_e$  are the intensity values at time  $t$ , zero, and equilibrium, respectively, and time was measured in seconds. The results of the experiments are reported in Table S-2 (Supporting Information) and also shown in Figure 6, where they are compared with similar data for the Nb(V) version of the molecule.<sup>4</sup>

There are several important features of the rate data for the  $[\text{H}_x\text{Ta}_6\text{O}_{19}]^{(8-x)-}$  molecule when compared with the  $[\text{H}_x\text{Nb}_6\text{O}_{19}]^{(8-x)-}$  ion. First, the overall reactivities of the two molecules are broadly similar. Second, the relative reactivities of the  $\eta=\text{O}$  and  $\mu_2\text{-O(H)}$  sites in the  $[\text{H}_x\text{Ta}_6\text{O}_{19}]^{(8-x)-}$  ion are opposite to those in the  $[\text{H}_x\text{Nb}_6\text{O}_{19}]^{(8-x)-}$  ion. For the  $[\text{H}_x\text{Nb}_6\text{O}_{19}]^{(8-x)-}$  ion in the range  $12.5 < \text{pH} < 14.5$ , the rates of isotopic exchange of the  $\eta=\text{O}$  and  $\mu_2\text{-O(H)}$  sites differ by about a factor of 10 from one another and the  $\eta=\text{O}$  sites react more slowly than the  $\mu_2\text{-O(H)}$  sites (Figure 6). For the  $[\text{H}_x\text{Ta}_6\text{O}_{19}]^{(8-x)-}$  ion in the same pH region, the  $\eta=\text{O}$  sites react about a factor of 10 more rapidly than the  $\mu_2\text{-O(H)}$  sites. Third, the pH dependencies of the rates for both the  $\eta=\text{O}$  and  $\mu_2\text{-O(H)}$  sites are distinctly different from

one another in the Ta(V) and Nb(V) versions of the molecules, although for both molecules, the rates in the region  $12.5 < \text{pH} < 14.5$  are largely independent of the pH. An additional difference is that the rates of isotopic exchange for the  $\mu_2\text{-O(H)}$  site in the  $[\text{H}_x\text{Nb}_6\text{O}_{19}]^{(8-x)-}$  molecule exhibit a slight pH dependence and eventually become equivalent in rate to the  $\eta=\text{O}$  site at  $\text{pH} \sim 14.5$  (Figure 6), whereas the rates for the  $[\text{H}_x\text{Ta}_6\text{O}_{19}]^{(8-x)-}$  molecule remain separate from one another at all conditions.

A profound pH dependence in the reaction rates, affecting both the  $\eta=\text{O}$  and  $\mu_2\text{-O(H)}$  sites, becomes evident at  $\text{pH} < 11.5$  for the  $[\text{H}_x\text{Ta}_6\text{O}_{19}]^{(8-x)-}$  ion and at  $\text{pH} < 12$  for the  $[\text{H}_x\text{Nb}_6\text{O}_{19}]^{(8-x)-}$  ion. For the  $[\text{H}_x\text{Nb}_6\text{O}_{19}]^{(8-x)-}$  ion, the rates of isotopic exchange of the  $\eta=\text{O}$  and  $\mu_2\text{-O(H)}$  sites converge as the pH drops. For the  $[\text{H}_x\text{Ta}_6\text{O}_{19}]^{(8-x)-}$  ion, the rates of isotopic exchange of the  $\eta=\text{O}$  and  $\mu_2\text{-O(H)}$  sites never converge but continue to differ by roughly 1 order of magnitude. It is particularly interesting that both the  $\eta=\text{O}$  and  $\mu_2\text{-O(H)}$  sites are labilized in both molecules as the pH drops. Both the structural data and the DFT calculations indicate that protonation of the  $\eta=\text{O}$  sites is always unfavored relative to the  $\mu_2\text{-O}$  sites. Apparently, when a  $\mu_2\text{-O}$  is protonated, the rates of isotopic exchange of all oxygens, except, of course, the inert  $\mu_6\text{-O}$ , increase.

## Discussion

**Rate Law.** The results described above indicate that the pathways for oxygen-isotope exchange at  $\eta=\text{O}$  and  $\mu_2\text{-O(H)}$  sites in the  $[\text{H}_x\text{Ta}_6\text{O}_{19}]^{(8-x)-}$  and  $[\text{H}_x\text{Nb}_6\text{O}_{19}]^{(8-x)-}$  Lindqvist ions are distinct from one another. These differences are striking in light of the considerable structural and electronic similarity between these two structures. Nevertheless, the rate data can be fit to the same general rate law that described the Nb(V) version of the molecule. Black et al.<sup>4</sup> used the following equation:

$$k_{\text{obs}} = \sum_{i=0}^2 k_i X_i \quad (4)$$

where, in this case,  $k_i$  indicates the rate constants and  $X_i$  is the mole fraction of each protonation stoichiometry (e.g.,  $x = 0-2$  in  $[\text{H}_x\text{Ta}_6\text{O}_{19}]^{(8-x)-}$ ). The mole fractions are given by

$$X_0 = \frac{[\text{Ta}_6\text{O}_{19}^{8-}]}{\sum [\text{H}_x\text{Ta}_6\text{O}_{19}^{(8-x)-}]}, \quad X_1 = \frac{[\text{HTa}_6\text{O}_{19}^{7-}]}{\sum [\text{H}_x\text{Ta}_6\text{O}_{19}^{(8-x)-}]},$$

$$X_2 = \frac{[\text{H}_2\text{Ta}_6\text{O}_{19}^{6-}]}{\sum [\text{H}_x\text{Ta}_6\text{O}_{19}^{(8-x)-}]}$$

where the subscripts refer to the number of protons on the  $[\text{H}_x\text{Ta}_6\text{O}_{19}]^{(8-x)-}$  ion. These mole fractions can be calculated from conditional equilibrium constants:

$$x_{\text{Ta}_6\text{O}_{19}^{8-}} = \frac{K_{a1}K_{a2}}{[\text{H}^+]^2 + [\text{H}^+]K_{a1} + K_{a1}K_{a2}}$$

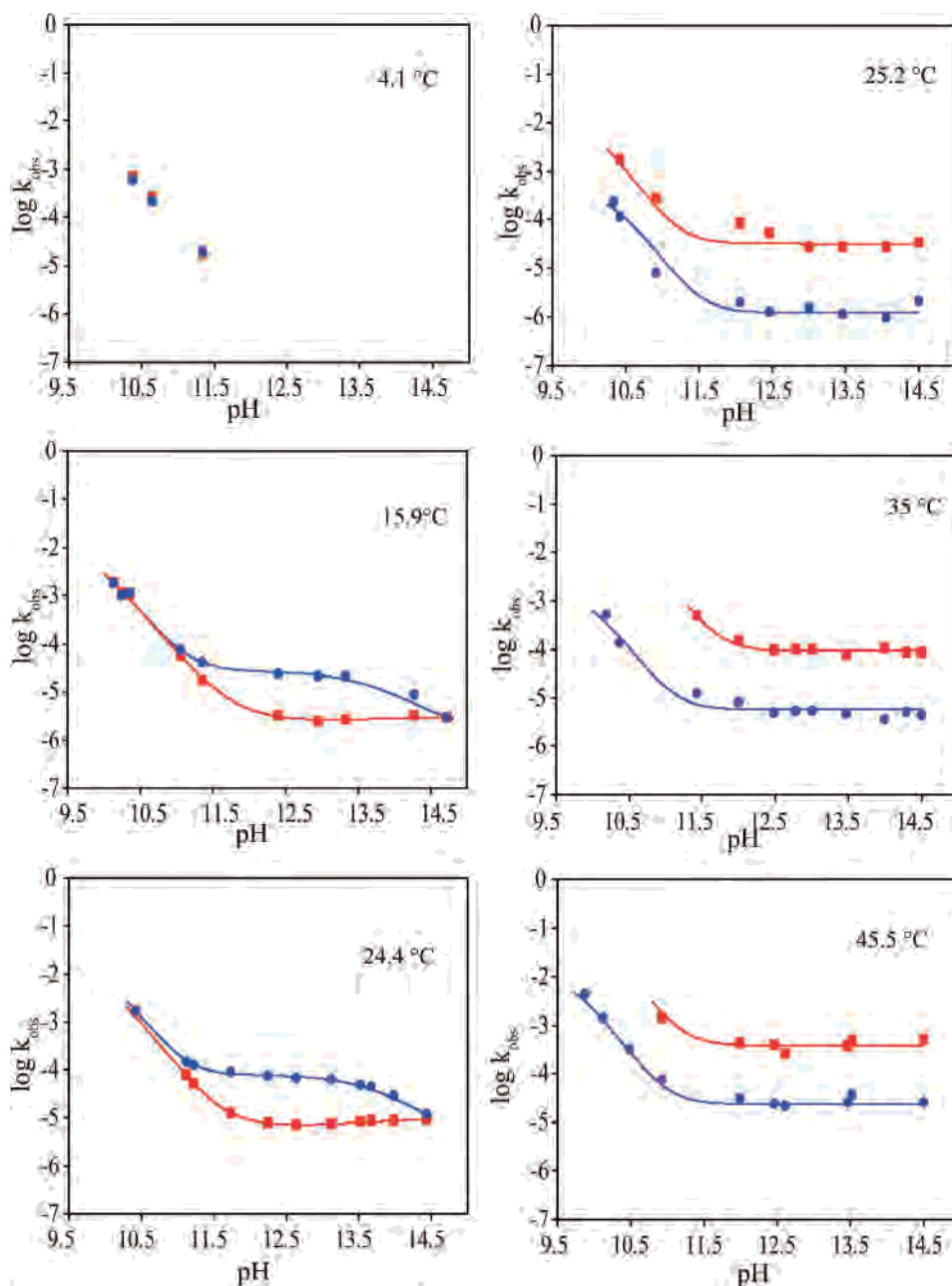


**Figure 6.** Rates as a function of the pH and temperature for the  $[\text{H}_x\text{Nb}_6\text{O}_{19}]^{(8-x)-}$  (left) and  $[\text{H}_x\text{Ta}_6\text{O}_{19}]^{(8-x)-}$  (right) Lindqvist ions. Data for the  $[\text{H}_x\text{Nb}_6\text{O}_{19}]^{(8-x)-}$  ion are from ref 4. The data for the  $\mu_2\text{-O(H)}$  sites are in blue circles, and the data for the  $\eta=\text{O}$  sites are in red squares. The lines correspond to fits of a rate law (eq 4) to the data.

$$x_{\text{Ta}_6\text{O}_{19}^{7-}} = \frac{K_{a1}[\text{H}^+]}{[\text{H}^+]^2 + [\text{H}^+]K_{a1} + K_{a1}K_{a2}}$$

$$x_{\text{H}_2\text{Ta}_6\text{O}_{19}^{6-}} = \frac{[\text{H}^+]^2}{[\text{H}^+]^2 + [\text{H}^+]K_{a1} + K_{a1}K_{a2}}$$

This rate law implies that the various protonated forms of the molecule contribute independently to the overall rate and that the incoming moiety is probably a water molecule and not a hydroxide or hydronium ion. Although this explanation is simple, we evaluated other models as well, including cases where the  $\text{p}K_a$  values were allowed to vary as adjustable parameters, where different protonated stoichiometries were

considered. The fitted rate constants, parameters, and residual errors are compiled in Table S-3 (Supporting Information).

The curve-fitting exercise yielded interesting results. First, inclusion of the  $\text{HTa}_6\text{O}_{19}^{7-}$  stoichiometry had practically no effect on the quality of the resulting fit (Table S-3 in the Supporting Information). Therefore, this stoichiometry was apparently not necessary to adequately fit the data. In contrast, excluding the  $\text{H}_2\text{Ta}_6\text{O}_{19}^{6-}$  stoichiometry always led to a much poorer fit. These fits, of course, are sensitive to the acid–base chemistry of the molecule, which is constrained only by our  $^{17}\text{O}$  NMR data because there are no independent estimates. We can think of no reasonable explanation for the absence of a monoprotated species and preference for the diprotated species, but the most interest-



**Table 1.** Activation Parameters for Oxygen-Isotope Exchange for Sites in the Ta(V) and Nb(V) Versions of the Lindqvist Ions<sup>32</sup>

	pH	$\eta=O$		$\mu_2-O$	
		$\Delta H^\ddagger$ (kJ·mol <sup>-1</sup> )	$\Delta S^\ddagger$ (J·K <sup>-1</sup> ·mol <sup>-1</sup> )	$\Delta H^\ddagger$ (kJ·mol <sup>-1</sup> )	$\Delta S^\ddagger$ (J·K <sup>-1</sup> ·mol <sup>-1</sup> )
Ta(V)	13	83.6 ± 3.2	-51.0 ± 10.6	70.3 ± 9.7	-116.1 ± 32.7
Nb(V)	~13	89.4	-42.9	88.0	-29.7

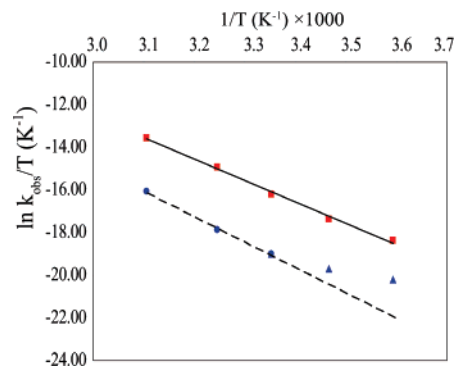
ing point is that protons at any site apparently labilize both  $\eta=O$  and  $\mu_2-O(H)$  sites. Nevertheless, we consistently found that varying the  $pK_a$  values had little effect on the value of  $k_0$ , corresponding to the  $Ta_6O_{19}^{8-}$  stoichiometry, while the higher values of  $k_2$  were highly sensitive to changes in the acid–base equilibrium, as one expects. In these fits, the deviations of  $pK_a$  from values determined from the NMR titration were in the range of 0.1–1 units. Although adequate fits could be achieved by adding an explicit dependence of the rate on  $[H_3O^+]$ , we excluded this model as unreasonable. At the high-pH conditions of these experiments, it is more reasonable to assume that water molecules are the isotopically exchanging moiety, as was concluded for the  $H_xNb_6O_{19}^{(8-x)-}$  ion by Black et al.<sup>4</sup>

At high pH, where the  $Ta_6O_{19}^{8-}$  stoichiometry dominates, there is no dependence of the rate on the solution pH. At these conditions, we could examine the temperature dependency of  $k_{obs}$  using the Eyring equation:

$$\frac{1}{k_{obs}} = \frac{k_B T}{h} e^{-(\Delta H^\ddagger - T\Delta S^\ddagger/RT)} \quad (5)$$

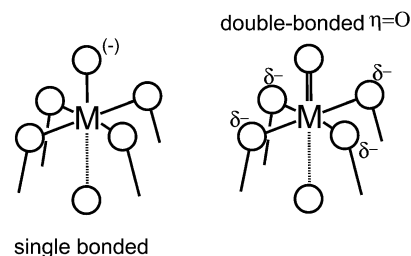
where  $k_B$  is Boltzmann's constants,  $h$  is Planck's constant,  $R$  is the gas constant, and  $T$  is the experimental temperature in Kelvin. The activation parameters are reported in Table 1, where they are compared to those of Black et al.,<sup>4</sup> for the  $Nb_6O_{19}^{8-}$  molecule at similar conditions. In estimating the activation parameters for the  $Ta_6O_{19}^{8-}$  molecule, we excluded two values at the lowest temperature because we suspected that the rate estimates were affected by  $CO_2$  uptake and pH drift (Figure 7). All data were included for the terminal peak, which reacted relatively quickly. (Experiments at higher temperatures are only a few dozen hours, whereas those at lower temperatures take weeks.) The solutions in these two samples had relatively low buffer capacity, and the rate experiments were particularly long, allowing  $CO_2$  to diffuse into the sample tubes.

**Pathways for Isotope Exchange.** In considering isotope-exchange reactions in the  $[H_xNb_6O_{19}]^{(8-x)-}$  ion, Black et al.<sup>4</sup> suggested that one of the three mutually orthogonal  $M_4(\mu_2-O)_4(\eta-O)_4$  rings opens to become a precursor to isotopic exchange. This pathway was appealing because  $\eta=O$  and  $\mu_2-O(H)$  sites in the Nb(V) Lindqvist ion sometimes react at equal rates and, in the ring-opened structure, the  $\eta=O$  and  $\mu_2-O(H)$  sites become temporarily equivalent. At this point, the Nb(V) metals also become undercoordinated and well-exposed to an incoming water molecule that can transfer protons and replace one of the structural oxygens. Black et al.<sup>4</sup> suggested that the ring-opened structure might actually

**Figure 7.** Temperature dependence of  $k_{obs}$  for the  $\mu_2-O$  (blue) and  $\eta=O$  (red) sites. The solid and dashed lines, respectively, correspond to fits of eq 5 to the data. The lowest-temperature points for the  $\eta=O$  site were excluded because these experiments were quite lengthy and we suspect that the rate estimates were affected by pH drift.

be a metastable form of the molecule, by analogy with other polyoxocations.<sup>29</sup>

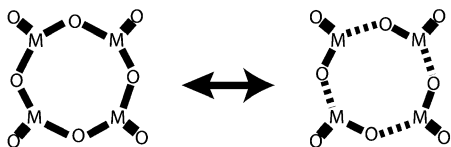
However, the  $\eta=O$  and  $\mu_2-O(H)$  rates for the  $[H_xTa_6O_{19}]^{(8-x)-}$  ion always differ from one another, and there is no need to invoke a mechanism that makes these two oxygens equivalent. Alternatively to the large-scale ring-opening mechanism of Black et al.,<sup>4</sup> the reaction could be at a single metal site, where  $\eta=O$  and  $\mu_2-O(H)$  within a  $Ta_4(\mu_2-O)_4(\eta-O)_4$  ring rotate and allow access of the water to the metal. The incoming water molecule can transfer protons to an outgoing structural oxygen, which leaves as a water molecule. The immediate analogy is isotopic exchange of a carbonyl oxygen in an ester.



A qualitative explanation for the differences in reactivities of isostructural Nb(V) and Ta(V) Lindqvist ions derives from the original work of Day and Klemperer,<sup>13</sup> who invoked two extreme resonance structures to explain the reactivities of  $\eta=O$  and  $\mu_2-O$  sites. In one structure, the pentavalent charge is distributed across five single bonds (the bond to the central  $\mu_6-O$  site is so long and weak as to be ignored), with the anion charge centered on the  $\eta=O$  site. For this structure, the terminal oxygens are expected to be more labile than the bridges, as we observe for the Ta(V) Lindqvist ion. An alternative form is a doubly bonded  $\eta=O$ , with bonds to bridging oxygens having bond orders less than unity;  $3/4$  bond orders would account for the 5+ metal charge. In this resonance structure, the terminal oxo is unreactive relative to the bridges, as we observe for the Nb(V) Lindqvist ion.

An alternative interpretation was generously suggested to us by Prof. Craig Hill and invokes alternating differences in

(29) Rustad, J. R.; Loring, J. S.; Casey, W. H. *Geochim. Cosmochim. Acta* **2004**, *68* (14), 3011–3017.



bond orders in the  $M_4(\mu_2\text{-O(H)})_4(\eta\text{-O})_4$  rings, by analogy with such quasi-conjugation in tungstates.<sup>30,31</sup> The essential idea is that the  $Nb_4(\mu_2\text{-O(H)})_4(\eta\text{-O})_4$  rings have a greater extent of alternating bond conjugation than the  $Ta_4(\mu_2\text{-O(H)})_4(\eta\text{-O})_4$  rings. This difference is manifested in a higher proton affinity (to the singly bonded oxygen in the ring) and the greater lability of one of the bridging oxygens as the ring opens for the niobate but not the tantalate.

We see no evidence in the electronic-structure calculations for differences in natural bond orders in the mutually orthogonal  $M_4(\mu_2\text{-O})_4(\eta\text{-O})_4$  rings that might suggest a heterogeneity in bonding to  $\mu_2\text{-O(H)}$  between the tantalate and niobate structures. There are small differences in natural bond order charges on the oxygens in the  $Ta_4(\mu_2\text{-O})_4(\eta\text{-O})_4$  and  $Nb_4(\mu_2\text{-O})_4(\eta\text{-O})_4$  rings, but these differences are inconsistent with the proton affinities and offer no clear suggestion of a pathway. Similarly, we see no evidence for bond conjugation in the  $M_4(\mu_2\text{-O})_4(\eta\text{-O})_4$  rings and have more extensive simulations underway. Coordinates and bond lengths are included in the Supporting Information.

## Conclusions

Oxygen-isotope-exchange rates were measured on the Ta(V) Lindqvist ions as a function of the pH and temperature, and these new data allow a useful comparison with the isostructural Nb(V) version. We find tantalizing differences in reactivities. First, the  $\eta\text{=O}$  oxygens in the Ta(V) molecule react faster than the  $\mu_2\text{-O(H)}$  oxygens, which is opposite to what is observed in the Nb(V) version molecule, where the  $\mu_2\text{-O(H)}$  oxygens react faster than the  $\eta\text{=O}$  oxygens in the range  $\sim 12 < \text{pH} < 14.5$ . Second, unlike in the  $H_xNb_6O_{19}^{(8-x)-}$  molecule, the  $\mu_2\text{-O(H)}$  and  $\eta\text{=O}$  oxygens in the  $H_xTa_6O_{19}^{(8-x)-}$  molecule never react at the same rates. Third, the activation parameters for the  $H_xNb_6O_{19}^{(8-x)-}$  and  $H_xTa_6O_{19}^{(8-x)-}$  suggest that the oxygen sites react via different pathways, in spite of the similarities of these molecules in electronic and physical structure. High-pressure NMR could be a useful tool to confirm these proposed differences in reaction mechanisms.

(30) Leclerc-Laronze, N.; Haouas, M.; Marrot, J.; Taulelle, F.; Herve, G. *Angew. Chem., Int. Ed.* **2005**, *45* (1), 139–142.

(31) Fang, X.; Hill, C. L. *Angew. Chem., Int. Ed.* **2007**, *46*, 1–5.

(32) Black, J. R.; Nyman, M.; Casey, W. H. *J. Am. Chem. Soc.* **2007**, *129* (16), 5298.

In both molecules, rates at both the  $\eta\text{=O}$  and  $\mu_2\text{-O(H)}$  sites increase as the molecules become protonated, which are probably at the bridging oxygens. This general labilization may be extraordinarily important for understanding reactions at extended oxide surfaces. Protonation of the  $\mu_2\text{-O}$  site is energetically favored by a few tens of kilojoules per mole relative to the  $\eta\text{=O}$  site but not equally so. The energy difference associated with moving a proton from a  $\mu_2\text{-OH}$  site to the  $\eta\text{=O}$  site on the  $H_xTa_6O_{19}^{(8-x)-}$  molecule is less than that for the  $H_xNb_6O_{19}^{(8-x)-}$  molecule by  $\sim 15 \text{ kJ}\cdot\text{mol}^{-1}$ , suggesting that protonation of the  $\eta\text{=O}$  site may be more involved in labilizing the molecule than that for the  $H_xNb_6O_{19}^{(8-x)-}$  ion. In general, proton affinities of oxygens on the  $H_xNb_6O_{19}^{(8-x)-}$  ion are greater than those for the corresponding site on the  $H_xTa_6O_{19}^{(8-x)-}$  ion, which is also evident in the experimental data.

These Lindqvist ions present interesting challenges to computation chemistry, as the comparison is so direct and fair. The fact that the oxygen sites react so unpredictably between these molecules suggests that models for site reactions at extended structures, for which data are more difficult to acquire, should be approached with caution. Our experience with aluminum polyoxocations<sup>11</sup> indicates that little can be understood definitively about the reaction pathways in a class of clusters until data are available for several compositions. Thus, we have experiments underway to synthesize and study the isotope-exchange reactions of other Lindqvist ions including  $[W_4Nb_2O_{19}]^{4-}$ .

**Acknowledgment.** The authors particularly thank Dr. Jay Black for advice and assistance. Support for this research was from the National Science Foundation via Grant EAR 05015600 and from the U.S. Department of Energy Office (DOE) of Basic Energy Science via Grants DE-FG03-96ER 14629 and DE-FG03-02ER15693. Support for M.N. was from the Sandia National Laboratories LDRD program. Sandia National Laboratories is a multiprogram laboratory operated by Sandia Corp., A Lockheed Martin Co., for the U.S. DOE under Contract DE-AC04-94AI85000. Spectrometers at the University of California at Davis NMR facility were purchased using funds from NSF Grant OSTI 97-24412.

**Supporting Information Available:** Electronic energies, isotopic exchange rates, results of the fit of the data to eq 4, bond lengths and angles, structures, and converged geometry coordinates. This material is available free of charge via the Internet at <http://pubs.acs.org>.

IC700845E